(2)

WSRL-TM-30/90

AR-006-454

A GENERIC INERTIAL NAVIGATION SYSTEM MODEL FOR COMPUTER SIMULATION STUDIES

D.A.B. FOGG and R.T. JANUS

COMBAT SYSTEMS DIVISION
WEAPONS SYSTEMS RESEARCH LABORATORY

Approved for Public Release.

SEPTEMBER 1990

DEPARTMENT OF DEFENCE
DEFENCE SCIENCE AND TECHNOLOGY ORGANISATION

UNCLASSIFIED

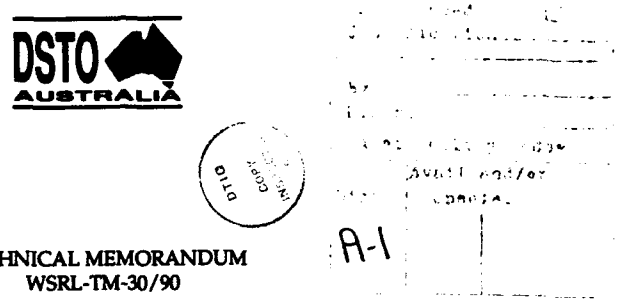

TECHNICAL MEMORANDUM
WSRL-TM-30/90

A GENERIC INERTIAL NAVIGATION SYSTEM MODEL FOR COMPUTER SIMULATION STUDIES

D.A.B. Fogg and R.T. Janus

SUMMARY (U)

A number of Inertial Navigation System (INS) models ranging from simple forced harmonic oscillator models to three-gyro, three-accelerometer systems were studied to ascertain a compromise between accuracy and computation time on the one hand and model complexity suitable for use in avionics system models for effectiveness studies on the other. INS position and orientation errors for various cruise and acceleration conditions were predicted by these models and the results shown graphically. The importance of various INS characteristics has been determined and the effects of the relevant error sources have been isolated and their propagation in time plotted.

Author's address:
Combat Systems Division
Weapons Systems Research Laboratory
PO Box 1700, Salisbury
South Australia

Requests to: Chief, Combat Systems Division

UNCLASSIFIED

TABLE OF CONTENTS

		Page
1.	INTRODUCTION	1
2.	COORDINATE SYSTEMS AND NOTATION CONVENTIONS	1
3.	INS CHARACTERISTICS	2
	3.1 Schuler tuning	2
	3.2 The Foucault effect	4
	3.3 Geographic latitude and longitude errors	4
	3.4 Gyroscope and accelerometer errors	5
4.	FORCED HARMONIC OSCILLATOR MODEL, MODEL M1	5
	4.1 Constant speed	6
	4.2 Constant linear acceleration	7
	4.3 Constant, centripetal acceleration	7
5.	TANGENT PLANE MODEL, MODEL M2	8
	5.1 Position error equations	9
	5.2 Platform error equations	11
6.	RESULTS AND COMPARISONS BETWEEN M1 AND M2, CRUISE CONDITIONS	11
	6.1 Variation of gyroscopic drift rate	11
	6.1.1 Position errors	12
	6.1.2 Platform errors	13
	6.2 The effects of initial velocity error	13

6.3 Initial misalignment error 13

6.3.1 Position error 13
6.3.2 Platform error 14

7. RESULTS AND COMPARISONS M1-M2, UNDER ACCELERATION 14

7.1 Constant linear acceleration 14

7.1.1 Position error 14
7.1.2 Platform errors 14

7.2 Constant centripetal acceleration 14

7.2.1 Position errors 14

7.2.2 Platform errors 15

8. COMPARISON OF MODEL M2 WITH MORE DETAILED MODELS 15

9. CONCLUSIONS AND RECOMMENDATIONS 16

NOTATION 18

REFERENCES 20

TABLE 1. CRUISE AND ACCELERATION PLATFORM PARAMETERS 17

LIST OF FIGURES

1. The variation in position error with gyroscopic drift rate 22

2. Comparison of M1-M2 radial position errors 23

3. The variation of platform error with gyro drift rate 24

4. Initial velocity error 25

5. Initial misalignment error 26

6. The effect of linear acceleration on position error 27

7. Comparison of M1-M2, radial position errors, under constant linear acceleration 28

8. The effect of linear acceleration on platform errors 29

9. The effect of centripetal acceleration on position error 30

10. A comparison of RMS latitude error for various flight directions 31

1. INTRODUCTION

The work described here is part of task AIR 86/166 to evaluate the performance of the F111-C Pave Tack system. This task involves the development of a digital computer performance model which necessarily encompasses a number of the F111-C avionics systems, namely those which significantly affect navigation and weapon delivery. Aircraft flight characteristics and the environment also need to be considered. The model is intended to examine many possible scenarios and options, and a deterministic approach is used, which implies that random decisions selected at numerous times during a simulation (ie a single run of the performance model) must be averaged by repetition. There is therefore a need to represent any system to be incorporated in the model in as simple a way as possible without compromising the accuracy of the overall model. One such system is the Inertial Navigation System (INS).

Mathematical models of generic and particular INS exist, see references 1 to 10. In simpler models, references 1 to 3, a constant drift in position error (radial) is considered to be adequate. Overall, models range from simple forced harmonic oscillators to detailed representations of the gyroscopes and accelerometers that comprise an INS, incorporating accurate representations of the sources and propagation characteristics of system errors.

Three generic models ranging from simple to detailed, were examined and compared. A simplified technique for representing radial aircraft position error in an INS was examined first. The next model was a two dimensional "tangent plane" system which predicted the longitudinal and lateral position errors as well as platform pointing errors. The third model examined was much more complex, incorporating the effect of geographic latitude and longitude, altitude, and better error representation.

The model is required to be suitably accurate while fast enough to be used as part of the overall Pave Tack performance model. The analysis of the improvement in navigational capability brought about by the use of Pave Tack requires an appraisal of the effect of acceleration on the INS. This aspect was critical in determining which of the three models examined was most suitable. Software was written for the first two models and specific flight conditions were examined. Comparisons were made between models one, two and the published results of model 3(ref.4). It is proposed to validate the chosen model at some later date, with respect to the effect of acceleration on INS error, by monitoring and recording aircraft position data obtained from aircraft instrumentation and comparing it with external radar tracking data.

2. COORDINATE SYSTEMS AND NOTATION CONVENTIONS

Three right-handed Cartesian coordinate systems are used namely:

(a) True axes OXYZ, are right-handed Cartesian with coordinates of any point denoted by (x,y,z). This system is fixed to the earth. The X-Y plane is tangential to the earth's surface at the origin, and the X-axis points north. Away from this base point the system axes are not locally level and will not in general point north.

(b) Platform axes $OX_pY_pZ_p$ fixed to the aircraft, origin at the INS origin. The positive OX-axis is aligned with the aircraft longitudinal axis and the positive Oz-axis is upward. The coordinates of any point are denoted by (x_p,y_p,z_p).

(c) Computed axes. The coordinates of any point are (x_c,y_c,z_c), representing the computed position or best estimate of (x,y,z).

The angular deviations between these three sets of coordinates are assumed to be small. They can be represented simply by angle vectors as follows:

$\underline{\phi}$ is the angle vector between true and platform axes.

$\underline{\delta\theta}$ is the angle vector between true and computed axes.

$\underline{\psi}$ is the angle vector between computed and platform axes.

Components of $\underline{\psi}$ are refered to as platform errors. Position errors, ie the differences between true and computed positions are represented by a subscript e, (eg x_e). Derivatives with respect to time are denoted by single or double dots respectively, over a symbol.

3. INS CHARACTERISTICS

In this section some phenomena associated with inertial navigation systems are considered in order to determine their relevance to the Pave Tack evaluation model.

3.1 Schuler tuning

An oscillatory mechanical system which is designed to sense the direction of the earth's gravitation is not affected by constant velocity. If however, it is subjected to a uniform acceleration it will in general indicate a shift from the true direction because it cannot distinguish between the applied acceleration and that due to gravity. Consider an accelerometer mounted on a servo controlled stable platform subject to gravitational acceleration g. If the platform is tilted by an angle θ the output a from the accelerometer is integrated twice (to determine θ) and is fed back to the servo to level the platform. If a uniform horizontal acceleration a_p is applied to the platform the output of the accelerometer is given by

$$a = a_p + g\sin\theta \tag{1}$$

and the servo adjusts the platform angle until

$$\frac{a_p}{g} + \sin\theta \approx \frac{a_p}{g} + \theta = 0 \tag{2}$$

so that the platform is no longer level. The tilt θ satisfies the relationship

$$\theta = -k \int \int a dt\, dt = -kg \int \int \theta dt\, dt \qquad (3)$$

where k is a constant. The equivalent differential equation is

$$\ddot{\theta} + kg\theta = 0. \qquad (4)$$

The solution(ref.16) is harmonic with period T and angular frequency ω given by

$$T = 2\pi/\sqrt{(kg)}$$

and

$$\omega = \sqrt{(kg)}.$$

Since the damping factor is zero the solution is oscillatory and can be written, denoting time by t, as

$$\theta = A \sin \omega t.$$

In general the centre of oscillation g_a differs from the true g direction. It can be shown(ref.4,13) that if k is the reciprocal of the earth's radius R, g_a coincides with g. The natural period of oscillation, denoted by T_s, becomes

$$T_s = 2\pi\sqrt{(R/g)} \qquad (5)$$

and an applied acceleration, or any arbitrary motion, will not change the centre of oscillation of the instrument. Taking $R = 6371 \times 10^3$ m and $g = 9.8062$ m/s^2 this period is found to be 84.4 min. The process of attempting to tune such an instrument to have a period T_s averaged over R and g in the area of operation is known as Schuler tuning. In practice the equivalent pendulum length achieved by this prosess is usually somewhat less than R.

An insight into this process is obtained by noting that the period of a simple pendulum is $2\pi\sqrt{(l/g)}$ where l is the pendulum length. If its period is T_s then l = R, the radius of the earth. A force causing horizontal acceleration of the pendulum platform acts on the point of support of the pendulum while g acts on the centre of gravity of the bob. If this coincided with the earth's centre, as it would if l = R, a horizontal acceleration of the platform would not disturb the pendulum swing.

A Schuler tuned system oscillates about true g with period T_s. Without Schuler tuning, under a horizontal platform acceleration, the system oscillates with period T about an erroneous centre of oscillation g_e and the resultant position error will oscillate with the same period. In addition the offset error (resulting from an accelerometer giving an output when there is no applied lateral acceleration) is proportional to t^2 without Schuler tuning. When the system has been Schuler tuned this error also oscillates with period T_s and is bounded.

3.2 The Foucault effect

If a simple pendulum suspended above the earth is started swinging in a definite vertical plane, this plane will rotate slowly about the vertical axis. Let Ω denote the angular velocity of precession relative to the earth and L_α the angle between the horizontal and the earth axis (ie geographical latitude, assuming the indicated and the actual gravitational directions are the same). Then the angular velocity of precession is given by, see reference 11,

$$\Omega = -\omega_E \sin L_\alpha \qquad (6)$$

where ω_E is the angular velocity of the earth.

In the northern hemisphere the direction of precession is clockwise (looking towards the centre of the earth) and anticlockwise in the southern hemisphere. At the equator Ω is clearly zero. At the poles $\Omega = \pm\omega_E$ and the pendulum's plane of swing remains constant in space while the earth turns beneath it. The period, or time for one complete precession cycle, clearly varies from one day to infinity. For example at latitude 45^0 the period will be $\sqrt{2}$ days or 34 hours. If the pendulum is observed with respect to a geographic reference system the projection of its oscillation on the x and y axes will appear as beat waves(ref.8) with short period proportional to $\sqrt{(R/g)}$ (Schuler) and long period proportional to $(\omega_E \sin L_\alpha)^{-1}$. For an INS system the Foucault effect on position errors is to modulate the Schuler oscillation at a frequency Ω. The amplitude, however, is second order and can be neglected in this study. For platform errors the Foucault modulation is a first order effect(ref.6). Fortunately the platform errors are of secondary importance for navigational purposes.

3.3 Geographic latitude and longitude errors

If the INS position errors are resolved into latitude and longitude rather than x_e and y_e, it can be shown(ref.6) that latitude error is of the form $(1 - \cos \omega_E)^{1/2}$ which is bounded (in the long term, eg over 24 hours) and that longitude error, which is of the form,

$$[\omega_E^2 t^2 + 2(1 - \cos \omega_E)^{1/2}] \quad (7)$$

is unbounded. However, for the first several hours the rate of increase of the latitude errors is greater than that of the longitude errors. This is supported by an analysis of operational data or drift rates of the AN/AJQ-20A INS fitted to the F111-C aircraft(ref.12) which quantifies this difference. Data from 584 IBNS flight data record cards were used for this purpose. The above is consistent with radial error (M1) and x_e and y_e (M2) being unbounded in general, as found in Sections 4 and 5. Latitude errors will also depend on whether the direction of flight is easterly or westerly. Further consideration is given to this matter in the next section.

3.4 Gyroscope and accelerometer errors

INS system errors arise from lack of perfection in the gyroscopes and accelerometers, and from errors in the initial values of INS parameters, such as alignment direction, position and velocity. Many errors of varying degrees of importance can be enumerated. They depend on the INS configuration (eg the number of gyros and accelerometers used) and the way in which the components are constructed and combined. For the purpose of this study (following reference 6) gyroscope drift rates ε_x', ε_y' and ε_z' were identified as well as drift rates ε_x'' and ε_y'' due to mass unbalance. The latter arises because of the inevitable slight misalignment of a gyroscope centre of gravity with its axis of support.

Of the many known accelerometer errors, bias and scale factor error(ref.4) were identified as the most significant and are incorporated into M2. Accelerometer bias is the mean acceleration indicated by the accelerometer when the actual input acceleration is zero. The response of an accelerometer to acceleration involves a scale factor, and the uncertainty in the value of this factor causes a steady state error in the prediction of acceleration. This error is proportional to the actual acceleration, and is called the scale factor error.

4. FORCED HARMONIC OSCILLATOR MODEL, MODEL M1

The differential equations derived for an inertial navigation system are in general coupled. However it has been shown(ref.5), that if the coupling terms (eg see equations (20) and (21)) are neglected, although the values of $x_e(t)$ and $y_e(t)$ obtained are different, a good first approximation to the radial error $[x_e^2(t) + y_e^2(t)]^{1/2}$ can be found. The decoupled equations can be written in the form:

$$\ddot{x}_e(t) + \omega_S^2 x_e(t) = F_1(t)$$

$$\ddot{y}_e(t) + \omega_S^2 y_e(t) = F_2(t) \quad (8)$$

where ω_S is the Schuler frequency and the $F_i(t)$ are arbitrary functions (accelerations) refered to as forcing functions. These equations are seen to be harmonic oscillators. For each equation the solution consists of two parts, the complementary function ($F_i(t) = 0$) and a particular integral dependent on the forcing function. These two parts are added to form the general solution to the equation. The complementary function is readily found to be

$$x_e(t) = x_e(0)\cos \omega_S t + (1/\omega_S)\dot{x}_e(0)\sin \omega_S t. \tag{9}$$

This is approximated well by

$$x_e(t) = x_e(0) + \dot{x}_e(0)t \tag{10}$$

since the Schuler frequency ω_S (see Section 3.1) is given by $\omega_S^2 = 1.6 \times 10^{-6}$ r/s, and therefore ω_S is very small allowing the approximation $\theta = \sin \theta$. A number of cases, distinguished by different forcing functions will be considered and the results will be compared with those from model M2.

4.1 Constant speed

In this case the aircraft on which the INS is mounted is flying straight and level at a constant speed. The forcing function is assumed to be a random variable A(t) with mean square value R_0 and an exponentially decaying autocorrelation function of the form $R_0 e^{-\alpha|t|}$. This yields a particular solution in the form of a mean square which, when averaged in time (denoted by the vinculum), becomes

$$\overline{x_{RMS}(t)} = (c_1 \alpha t + c_0)^{1/2} \tag{11}$$

where,

$$c_1 = R_0 / \{\omega_S^2(\alpha^2 + \omega_S^2)\}$$

and

$$c_0 = c_1\{2\omega_S^2/(\alpha^2 + \omega_S^2) - 1/2\}.$$

4.2 Constant linear acceleration

Consider the application of a step of magnitude a in acceleration along the aircraft longitudinal axis for a duration d seconds from time t_1 to t_2 while the aircraft is flying straight and level at constant speed. The assumption is made(ref.5), that the forcing function in the error is proportional to the forcing function for the position coordinate x(t). Denoting the unit step function by U(t), and the constant of proportionality by k, the forcing functions can be written:

$$F_1(t) = ka\{U(t - t_1)-U(t - t_2)\}$$

$$F_2(t) = 0. \qquad (12)$$

The particular integral for the equation in $x_e(t)$ is readily found to be

$$x_e(t) = \frac{ka}{\omega_S^2}\,[\{1 - \cos \omega_S(t - t_1)\} - \{1 - \cos \omega_S(t - t_2)\}], \quad t > t_2 > t_1. \qquad (13)$$

Using trigonometrical transformations this can be written, using d in place of $t_2 - t_1$ as

$$x_e(t) = \frac{2ka}{\omega_S^2}\,\sin[\omega_S\{t - \tfrac{1}{2}d\}]\,\sin(\tfrac{1}{2}\omega_S d)$$

or, since ω_S is small,

$$x_e(t) = kad(t - \tfrac{1}{2}d). \qquad (14)$$

4.3 Constant, centripetal acceleration

If while flying straight and level at constant speed, the aircraft commences a constant centripetal acceleration turn (ie circular motion in the horizontal plane) of magnitude ng, the x and y components of the force are -ng cos α and ng sin α respectively. Where α is measured anticlockwise from the y-axis.

The angular velocity is given by $\omega = ng/v$ so that the forcing functions are given by:

$$F_1(t) = -k_1 \sin(ngt/v) \tag{15}$$

$$F_2(t) = k_1 \cos(ngt/v) \tag{16}$$

where k_1 is the amplitude of the forcing oscillation. The particular solutions for this type of forcing function are well known(ref.11), to be:

$$x_e(t) = \frac{-ng}{\omega_S^2 - \omega^2} \cos \omega t \tag{17}$$

$$y_e(t) = \frac{ng}{\omega_S^2 - \omega^2} \sin \omega t. \tag{18}$$

These solutions are compared with those of model M2 in the next section. The constants k, k_1 in this section and in Section 4.2 need to be determined empirically or by comparison with a better model.

5. TANGENT PLANE MODEL, MODEL M2

Model M2 is derived in reference 4. There are a number of comparable models in the literature, references 5 to 8. The error sources considered in this model include:

accelerometer bias,
accelerometer scale factor,
inherent gyro drift rate,
gyro mass unbalance drift rate,
initial platform misalignment,
initial position errors, and
initial velocity errors.

In general the INS alignment procedure undergone before an aircraft takes off implies a correlation between the initial position and initial velocity errors(ref.4). This has not been included but will not affect the conclusions drawn here.

5.1 Position error equations

The radial position error, (ie the vector sum of errors in the level, nominally horizontal, plane) is denoted by $\underline{r}_e$. It satisfies the equation(ref.4),

$$\ddot{\underline{r}}_e(t) + \omega_S^2 \underline{r}_e(t) = -[\underline{\psi}(t) \times \underline{A}(t)]_r + [\underline{A}_e]_r \qquad (19)$$

where $\underline{A}$ is the accelerometer signal, $\underline{A}_e$ is its error and the level component of $\underline{A}_e$ is denoted by $[\cdot]_r$. The resemblance to equations (8) is clear. The solutions will again oscillate with Schuler frequency ω_S. The vector product in the first of the terms on the right hand side of equation (19) is the error in sensing $\underline{A}$ resulting from the misorientation $\underline{\psi}$. The term $\underline{A}_e$ includes the accelerometer bias and scale factor. This equation can be resolved into x_e and y_e components to obtain the INS position errors for a cruising vehicle, namely

$$x_e(t) = x_e(0)\cos\omega_S t + \dot{x}_e(0)\frac{\sin\omega_S t}{\omega_S} - \psi_y(0)\,R(1-\cos\omega_S t) +$$

$$\psi_z(0)v_y t + \frac{B_x}{\omega_S^2}(1-\cos\omega_S t) - \left[K_x v_x + \frac{\varepsilon'_y g}{\omega_S^2}\right]\left[t - \frac{\sin\omega_S t}{\omega_S}\right]$$

$$+ \varepsilon'_z v_y\,[t^2 - 2/\omega_S^2(1-\cos\omega_S t)] - \tfrac{1}{2}\varepsilon''_y g v t^2 \qquad (20)$$

$$y_e(t) = y_e(0)\cos\omega_S t + \dot{y}_e(0)\frac{\sin\omega_S t}{\omega_S} + \psi_x(0)\,R(1-\cos\omega_S t) -$$

$$\psi_z(0)v_x t + \frac{B_y}{\omega_S^2}(1-\cos\omega_S t) - \left[K_y v_y + \frac{\varepsilon'_x g}{\omega_S^2}\right]\left[t - \frac{\sin\omega_S t}{\omega_S}\right]$$

$$- \varepsilon'_z v_x\,[t^2 - 2/\omega_S^2(1-\cos\omega_S t)] + \tfrac{1}{2}\varepsilon''_x g v t^2 \qquad (21)$$

where $\underline{B}$ is the accelerometer bias,

K_x, K_y are accelerometer scale factors,

g is the acceleration due to gravity,

R is the earth's radius,

v_x, v_y are the components of v in the true reference frame,

$\varepsilon'_x, \varepsilon'_y, \varepsilon'_z$ are inherent gyro drift rates, and

$\varepsilon''_x, \varepsilon''_y$ are gyro drift rates due to mass unbalance.

It should be noted that dimensional analysis of the above equations as presented in reference 4 (equation 7.29) indicated discrepancies. These were taken to be typographical errors. The equations shown above were derived from earlier work in reference 4 and are dimensionally correct. The above expressions can be evaluated directly to determine the error in x and y for a given set of initial conditions. The variables and constants used in the evaluation are defined in Table 1 together with their initial values. These equations involve general acceleration terms. When dealing with cruise conditions, $\ddot{x}$ and $\ddot{y}$ are assumed to be impulses at launch (t = 0) and zero after t = 0. To determine the position error when $\ddot{x}$ and $\ddot{y}$ are not constant with time, the following differential equations need to be solved:

$$\ddot{x}_e(t) + \omega_S^2 x_e(t) = -\psi_y(0)g + \psi_z(0)\,(\ddot{y}(t) + \omega_S^2 v_y t) + B_x - K_x\omega_S^2 v_x t$$

$$- \varepsilon'_y g t + \varepsilon'_z t\,[\ddot{y}(t) + \omega_S^2 v_y t] - \varepsilon''_y (v + \tfrac{1}{2}\omega_S^2 v t^2) g \qquad (22)$$

$$\ddot{y}_e(t) + \omega_S^2 y_e(t) = \psi_x(0)g - \psi_z(0)\,(\ddot{x}(t) + \omega_S^2 v_x t) + B_y - K_y\omega_S^2 v_y t$$

$$- \varepsilon'_x g t + \varepsilon'_z t\,[\ddot{x}(t) + \omega_S^2 v_x t] + \varepsilon''_x (v + \tfrac{1}{2}\omega_S^2 v t^2) g. \qquad (23)$$

The software to solve these equations accommodates general definitions of $\ddot{x}(t)$ and $\ddot{y}(t)$ in the form of complete sets of values specified at the integration interval.

5.2 Platform error equations

The INS platform errors(ref.4), are treated in a similar fashion. Assuming the horizontal acceleration $\dot{v}(t)$ to be an impulse at launch and the velocity v(t) to be constant for $t > 0$, the expressions for the platform errors are:

$$\psi_x(t) = \psi_x(0) + \varepsilon_x' t + \varepsilon_x'' (v + \tfrac{1}{2}\omega_S^2 v t^2)$$

$$\psi_y(t) = \psi_y(0) + \varepsilon_y' t + \varepsilon_y'' (v + \tfrac{1}{2}\omega_S^2 v t^2)$$

$$\psi_z(t) = \psi_z(0) + \varepsilon_z' t. \qquad (24)$$

In the cases where $\dot{v}(t) \neq 0$ for all $t \neq 0$ the following equations need to be solved:

$$\dot{\psi}_x(t) = \varepsilon_x' t + \varepsilon_x'' (\dot{v} + \omega_S^2 v t)$$

$$\dot{\psi}_y(t) = \varepsilon_y' t + \varepsilon_y'' (\dot{v} + \omega_S^2 v t)$$

$$\dot{\psi}_z(t) = \varepsilon_z'. \qquad (25)$$

The initial conditions pertaining to equations (24) and (25) are also shown in Table 1.

6. RESULTS AND COMPARISONS BETWEEN M1 AND M2, CRUISE CONDITIONS

6.1 Variation of gyroscopic drift rate

In M2 the gyroscopic drift rate ε' is assumed to have a constant value which would be determined by observation or from the INS specifications. It is shown below that it is clearly important to ascertain the correct value of the gyro drift rate to be able to correctly estimate the errors in a given INS system. M2 is preferred to M1 for long term simulation of radial position error due to gyro drift rate.

6.1.1 Position errors

Using model M2, the variation in position error with time is shown for four different values of the drift rate, namely 0.01, 0.1, 1.0 and 10.0 ^{o}/h, in figure 1 where $\log_{10}x_e(t)$ is plotted against $\log_{10}t$. In this model ε'_x and ε'_y are assumed to be identical. The modulation on these curves is due to Schuler oscillation (see Section 3.1). The local maxima/minima in this modulation occur when $\dot{x}_e(t)=0$. From equation (20) it can be seen that this is dependent on the initial conditions $x_e(0)$, $\dot{x}_e(0)$, $\psi_y(0)$, $\psi_z(0)$ and the values of ε'_y, ε'_z, ε''_y. This accounts for the different phases in the Schuler cycle seen from curve to curve.

No graphs showing error versus gyro drift rate were shown since at any given time t_1 the dependence of x_e in the absence of this modulation is linear, ie

$$x_e(\varepsilon'_y)_{t=t1} = g\varepsilon'_y/\omega_S^2 + c \tag{26}$$

where c is a constant.

The form of the corresponding error functions in M1 (RMS error) before logarithmic scaling is a parabolic section (equation (11)) with axis parallel to the time axis and focus at the point

$$\left[\frac{c_1^2\alpha^2 - 4c_0}{4c_1\alpha}\ ,\ 0\right].$$

Taking logarithms to base 10, equation (11) becomes,

$$\log_{10}x_{RMS}(t) = \tfrac{1}{2}\log_{10}(c_1\alpha t + c_0) \tag{27}$$

and since $c_0 = -\frac{1}{2}c_1$, this can be written

$$\log_{10}x_{RMS}(t) = \tfrac{1}{2}\log_{10}c_1 + \tfrac{1}{2}\log_{10}(\alpha t - \tfrac{1}{2}), \quad \alpha t > \tfrac{1}{2}. \tag{28}$$

The graph of this, using a log-log scale is linear in the time region of interest. Since the slope is fixed at $\frac{1}{2}$, a reasonable match with the results of M2 is only possible over the first several minutes. An example is shown in figure 2. The values of α and R_0 must be determined empirically or by

error plots from M1 and M2. R_0 and α were varied until a reasonable match was obtained. A slightly better match could be obtained by least squares fitting but was considered unwarranted for this illustration.

6.1.2 Platform errors

Using the initial and operating conditions of Block 7 in Table 1 again, the solutions for platform errors ψ_x and ψ_y were obtained. These are identical in M2. Error plots are shown in figure 3 for both the cruise condition and a 3 g lateral acceleration and drift rates from 0.01 to 1.0 ^{o}/h. The difference between the accelerated and unaccelerated values were found to follow the same time curve for all drift rate values. The errors under acceleration x_e, and without acceleration x_e' are related by

$$x_e(t) - x_e'(t) = C(g)t \tag{29}$$

where C(g) is a constant for a given g. This effect has been discussed further in Section 3.5. The M1 model does not estimate platform errors.

6.2 The effects of initial velocity error

In this section the effect of the initial velocity errors $\dot{x}_e(0)$, $\dot{y}_e(0)$ on the position error predicted by M2 is examined. Note that platform error, equations (24) and (25), is not dependent on these initial velocity errors. In figure 4 the values from Block 1 in Table 1 are used except that the initial value of $\dot{x}_e(0)$ is varied from 0.3 m/s to 5 m/s and 10 m/s, and $\varepsilon_x' = \varepsilon_y' = 0.01$ ^{o}/h (the $\dot{y}_e(0)$ analysis is identical). The three position error plots are shown against time on a log-log scale. For the first 40 min there is no correspondence, but after that the curves approach each other asymptotically.

6.3 Initial misalignment error

Initial misalignment error terms $\psi_x(0)$, $\psi_y(0)$, $\psi_z(0)$ in M2 propagate into both the position and platform error predictions.

6.3.1 Position error

Three values of misalignment error 10, 100 and 1000 arcsec (ie 0.05, 0.5 and 50.0 mrad) are used together with a gyro drift rate of 0.01 ^{o}/h. (See Table 1, Blocks 1, 3 and 4 for the parameter values used). The effect of an initial error in alignment is seen to be significant and long lasting,see figure 5.

6.3.2 *Platform error*

It can be seen from the platform error equations (24) that the initial alignment errors are simply additive constants and effect the origin but not the slope of the linearly increasing platform errors. The values of 100 and 1000 arcsec are very large compared to the increase in platform error with time (eg 50 s). Since graphs of these quantities would effectively be straight lines they have not been plotted. The 10 arcsec case is discussed under Section 7.1.2 and a graph of the corresponding platform error versus time is shown for reference with platform errors under acceleration.

7. RESULTS AND COMPARISONS M1-M2, UNDER ACCELERATION

Both longitudinal (along aircraft roll axis) lateral (along aircraft pitch axis) and centripetal accelerations were examined. In M1 and M2, lateral and longitudinal acceleration give rise to errors of the same magnitude.

7.1 Constant linear acceleration

7.1.1 *Position error*

The effects of constant acceleration (longitudinal or lateral) varying from 0.5 g to 3 g are shown in figure 6. The error without acceleration and the differences between the two are shown. They are only plotted for 50 s as this is long enough to indicate the effects of such accelerations.

A comparison of radial errors for M1 and M2 under constant acceleration is shown in figure 7. Although the error in M2 is clearly non-linear the M1 error is given by equation (14) which is linear. The value of k for this model has to be determined. The least squares technique was used to ascertain its value for figure 7 where an acceleration of 3 g was applied for 50 s ($k = 4.49 \times 10^{-5}$).

7.1.2 *Platform errors*

In figure 8 platform errors are shown for linear accelerations of 0.5 g to 3 g. Drift rates are seen to be from 2.0×10^{-6} to 3.1×10^{-6} r/s or 24 to 38 arcsec/min compared to 21.8 arcsec/min for the postulated unaccelerated INS.

7.2 Constant centripetal acceleration

7.2.1 *Position errors*

A series of graphs illustrating the effect of constant centripetal acceleration are shown in figure 9. The reference graph for the unaccelerated case is also shown, as are the differences between the accelerated and unaccelerated cases. Oscillation of the error as the platform is flown through successive complete circles can be seen. Using the relationship for radial velocity $v^2/r = ng$, where r is the radius of turn and n is the lateral acceleration (constant) in multiples of the acceleration due

to gravity, g, the turn duration is given by $t = s/v$ (where s is distance around the circular path) and the duration of one complete turn is readily shown to be $t = 2\pi v/ng$. For the 3 g, v = 300 m/s case used for figure 9, t = 64.1 s. The error is seen to oscillate with this period.

Equations (17) and (18) representing position error in M1 under centripetal acceleration are again linear over the time interval shown in figure 9. A graph of this is not shown. The slope could be determined empirically or by comparison with a better model, eg M2. The maximum difference in predicted error between M1 and M2 would be half the maximum error between the M2 graph and the reference (unaccelerated) case.

7.2.2 Platform errors

It can be seen from equations (25) that the platform errors, dependent only on $\dot{v}$ are the same for both the linear and the centripetal acceleration cases (figure 8).

8. COMPARISON OF MODEL M2 WITH MORE DETAILED MODELS

Possible improvements to M2 include the use of a reference axes system based on latitude L_α, longitude L_0 and altitude A. A number of models which use the $OL_\alpha L_0 A$ frame of reference were considered(ref.4 to 8) and an attempt was made to consider the trade-off between more accurate representation of the INS errors and increased complexity/computing time of these models compared to M2. In reference 6 the expression derived for the error in latitude L_e in response to white noise is

$$\bar{L}_e^2 = \frac{N}{2\dot{\lambda}^3}\left(\dot{\lambda}t - \frac{1}{2}\sin 2\dot{\lambda}t\right) \qquad (30)$$

where N is a constant gyro drift rate power spectral density function (≈ 1 arc min^2/h^3) and $\dot{\lambda}$ is celestial longitude rate. Figure 10 shows the RMS error (the square root of the expression in equation (30)) as a function of time for :

(1) westerly flight at latitude 35° and 300 m/s,

(2) at earth rate (15 °/h), the stationary case ($\dot{L}_0 = 0$), and

(3) easterly flight at latitude 35° and 300 m/s.

The difference between these cases starts to become significant after about two hours, indicating that a model that does not take the geographical direction into account should not be relied on after this length of time.

When the INS platform is subject to vertical acceleration and/or vertical velocity, the computations are inherently unstable because of the variation of gravity with altitude(ref.7). A weighted combination of altimeter and INS computed altitude can be used to deal with this problem. Models incorporating this effect have been examined(ref.4 to 8). They were considered to be beyond the scope of the current task for which the INS model was intended, namely to assist in the evaluation of the Pave Tack system.

These considerations indicate that M2 would become inadequate after 2 hours of simulated run time, and would have to assume a knowledge of altitude from some other source. From this examination of $OL_{\alpha}L_{0}A$ based models it was considered that the increase in computational complexity and the corresponding increase in computing time compared to M2 were not warranted.

9. CONCLUSIONS AND RECOMMENDATIONS

The characteristics of INS systems including gyro and accelerometer errors, initial alignment and other initialisation errors, the Schuler and Foucault cycles and the altitude prediction problem have been considered for inclusion in an INS model suitable for use in the evaluation of the F111-C Pave Tack system. Three types of model varying from simple forced harmonic oscillators to detailed three-gyro, three-accelerometer systems were considered and compared.

A "tangential plane" model M2 was found to give suitably reliable predictions of INS position and orientation errors for up to two hours flight time under cruise conditions, while satisfying time and complexity restrictions imposed by its intended role in an F111-C Pave Tack effectiveness model. In addition the model was able to predict the effects of linear and centripetal accelerations on these errors. INS predictions for a range of cruise and acceleration conditions have been produced for use in the Pave Tack task. The rates of propagation of various types of error with time were also demonstrated graphically. No empirical data were available to check the predictions of errors under acceleration, nor were they generally available from any published theoretical analyses or manufacturers' specifications.

It is recommended that suitable records of INS output and aircraft flight position from external tracking instruments be obtained during F111-C trials to validate the model, particularly the errors under acceleration.

TABLE 1. CRUISE AND ACCELERATION PLATFORM PARAMETERS

The term Block is used to refer to sets of input data.

The following parameters are used for all Blocks: ε_x' runs through 0.01, 0.1, 1.0, 10.0, $\varepsilon_y' = \varepsilon_x'$, $\varepsilon_z' = 0.01$, speed = 400 m/s.

For Blocks 1 to 5, acceleration is 0 m/s^2.

Initial Velocity Error $\dot{x}_e(0)$, $\dot{y}_e(0)$ Misalignment Error $\psi_x(0)$, $\psi_y(0)$	0.3 m/s	5 m/s	10 m/s
10 arcsec (0.05 mrad)	BLOCK 1	BLOCK 2	BLOCK 3
100 arcsec (5 mrad)	BLOCK 4		
1000 arcsec (50 mrad)	BLOCK 5		

BLOCK 6
ACCELERATION RUNS THROUGH 0.5 g, 1 g, 2 g, 3 g.
$\varepsilon_x' = \varepsilon_y' = \varepsilon_z' = 0.01$ °/hr, speed = 400 m/s
$\dot{x}_e(0) = \dot{y}_e(0) = 0.3$ m/s
$\psi_x(0) = \psi_y(0) = 0.05$ mrad

BLOCK 7
Acceleration 3 g (lateral or longitudinal as required)
ε_x', ε_y' run through 0.01, 0.1, 1.0, 10.0, $\varepsilon_z' = 0.01$
$\dot{x}_e(0) = \dot{y}_e(0) = 0.3$ m/s
$\psi_x(0) = \psi_y(0) = 0.05$ mrad

NOTATION

$\underline{A}$	Acceleration signal vector
B_x, B_y	Components of accelerometer bias
c, c_0, c_1	Constants
k	Constant
K_x, K_y	Components of scale factor
$\underline{r}$	Position error vector
R	Earth radius
g	Acceleration due to gravity
t	Time
v	System velocity
v_x, v_y, v_z	System velocity components, true coordinates
x, y, z	True position coordinates
x_c, y_c, z_c	Computed position coordinates
x_e, y_e, z_e	Errors between true and position coordinates
$\underline{\delta\theta}$	The angle vector between true and computed axes
$\varepsilon_x', \varepsilon_y', \varepsilon_z'$	Constant gyro drift rate components
$\varepsilon_x'', \varepsilon_y'', \varepsilon_z''$	Gyro drift rate components due to mass unbalance
θ	general angle
λ	celestial longitude
ϕ_x, ϕ_y, ϕ_z	Components of the angle vector between true and platform axes
Ψ_x, Ψ_y, Ψ_z	Components of the angle vector between computer and platform axes

$\omega_0, \omega_p, \omega_c$	The angular rates of true, platform and computed axes with respect to inertial space, respectively
ω_E	Angular velocity of the earth
ω_S	Schuler frequency
$\dot{}, \ddot{}$	First and second derivatives with respect to time

REFERENCES

No.	Author	Title
1	-	"System Segment Specification for the F111 A/E Avionics Modernisation Program". 32SSV001, 3, April 1986
2	-	"F111 A/E AMP Navigation and Weapon System Error Analysis". Grumman Aerospace Corporation. AMPRPT-86-003, 12 April 1986
3	Fogg, D.A.B. and Lukacs, S.	"An Analysis of Navigation and Weapon Delivery Accuracy for the F111-C Avionics Update, Part I, Procedures and Summary of Results (U)". Technical Report, WSRL-TR-17/89, March 1989
4	Pitman, G.R. Jr	"Inertial Guidance". John Wiley & Sons, New York, 1962
5	Savant, C.J. Jr, Howard, R.C., Solloway, C.B. and Savant, C.A.	"Principles of Inertial Navigation". McGraw Hill, New York, 1961
6	Britting, K.R.	"Inertial Navigation Systems Analysis". Wiley Interscience, New York, 1971
7	Fernandez, M. and Macomber, G.R.	"Inertial Guidance Engineering". Prentice Hall, Englewood Cliffs, NJ, USA, 1962
8	Broxmeyer, C.	"Inertial Navigation Systems". McGraw Hill, New York, 1964
9	Lloyd, I.V.	"A Simple Error Model for Inertial Navigation Systems". Group Report SOG 13, Aeronautical Research Laboratories, Melbourne, April 1975
10	-	"Fin 1100, Error Model Program NSD 5564". Issue 11, Ferranti, Navigation Systems Department, Edinburgh, Scotland, December 1984

11	Symon, K.R.	"Mechanics". Addison Wesley, Reading, USA, 1960
12	Gazley, J.G.	"F111-C Inertial Navigation System Performance". 25/2/Air, November 1974
13	Schuler, M.	"The Disturbance of Pendulum and Gyroscopic Apparatus by the Acceleration of the Vertical". Physikalische Zeitschrift Vol.24, July 1923 (Translation in reference 4)
14	Broxmeyer, C.	"Foucault Pendulum Effect in a Schuler Tuned System". Journal Aerospace Science, Vol.27, No.5, May 1960
15	Wrigley, W.	"Schuler Tuning Characteristics". Navigation Instruments, Vol.2, No.8, December 1950
16	Korn, G.A. and Korn, T.	"Mathematical Handbook for Scientists and Engineers". McGraw-Hill, 1976

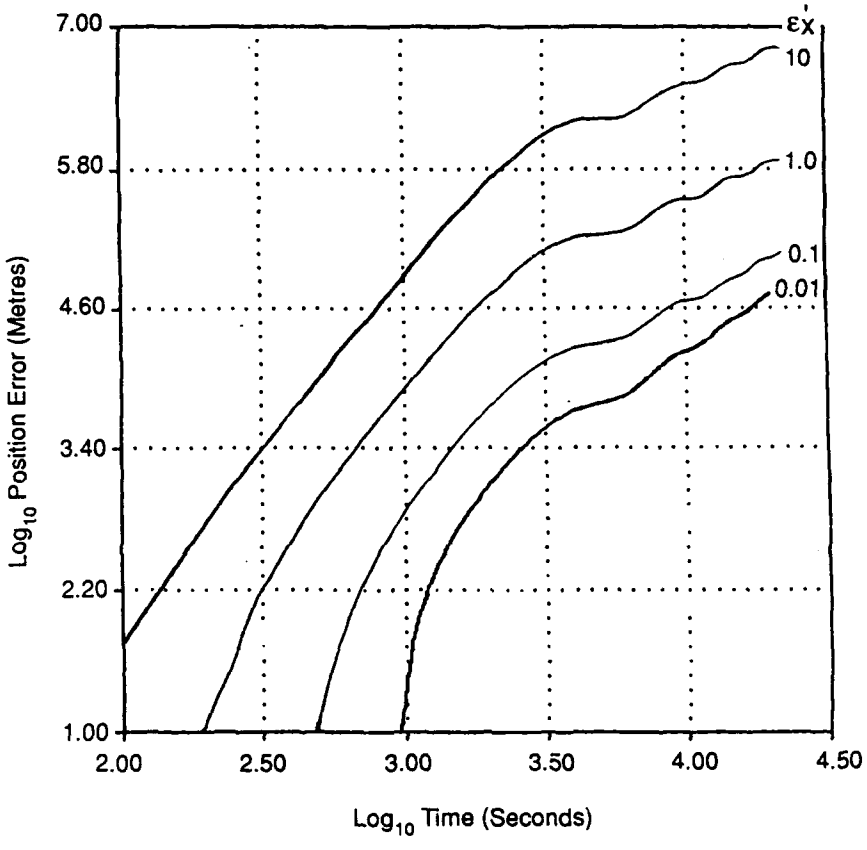

Figure 1. The variation in position error with gyroscopic drift rate

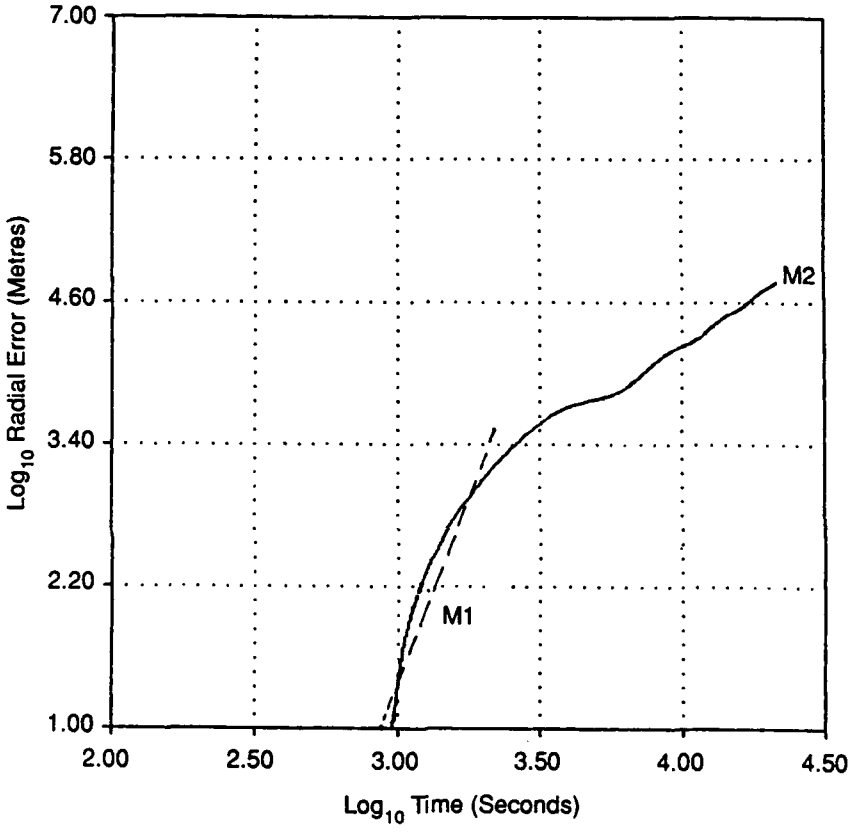

Figure 2. Comparison of M1-M2 radial position errors

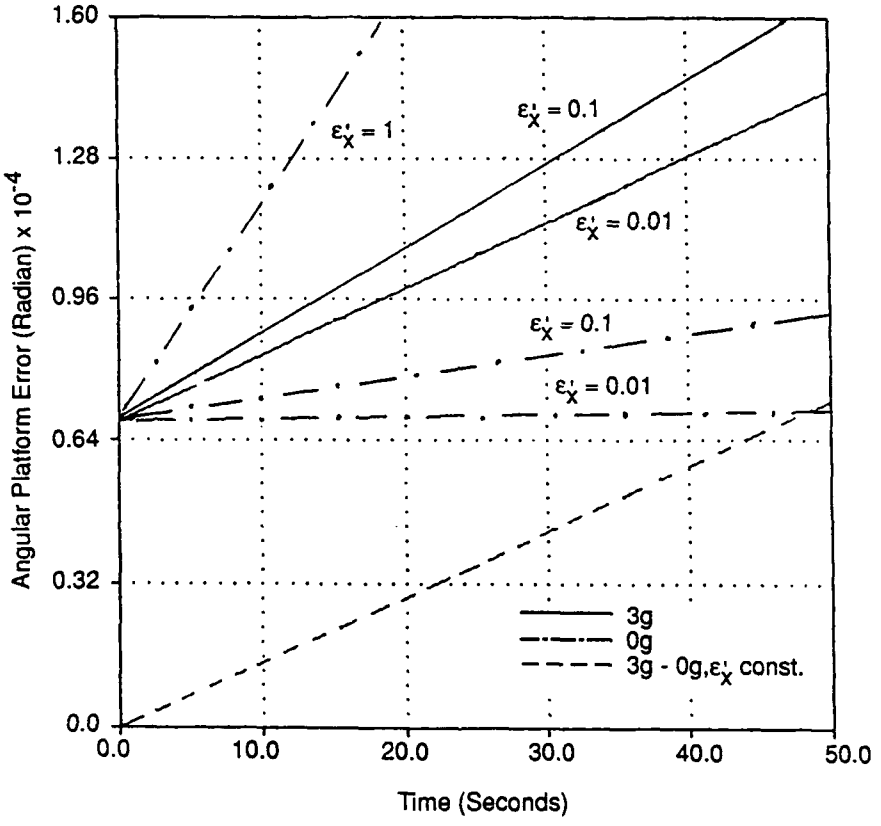

Figure 3. The variation of platform error with gyro drift rate

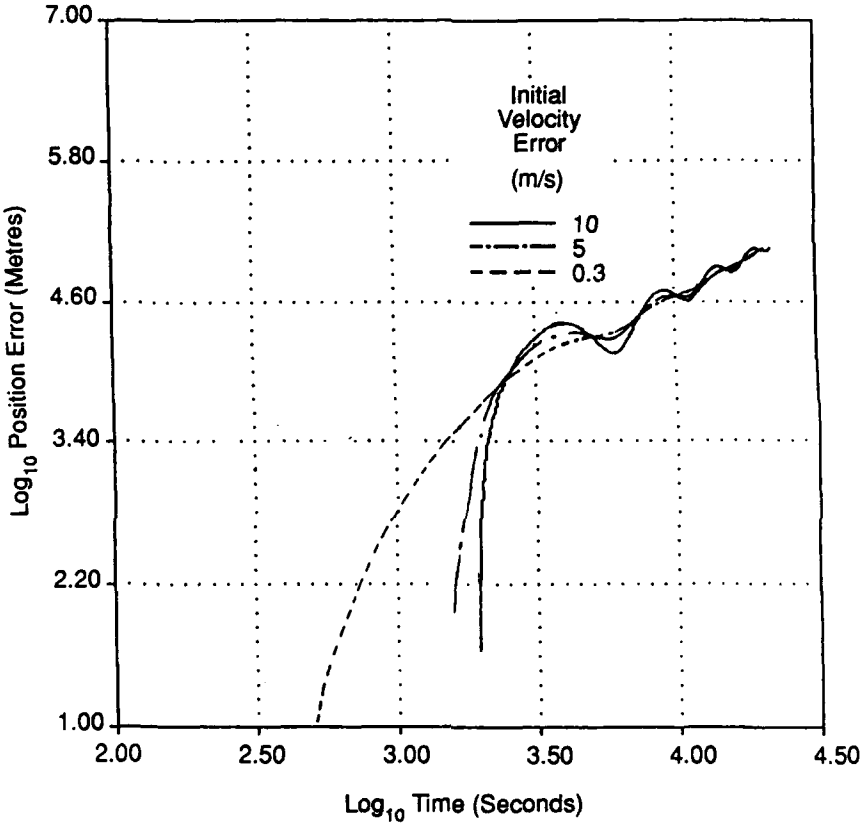

Figure 4. Initial velocity error

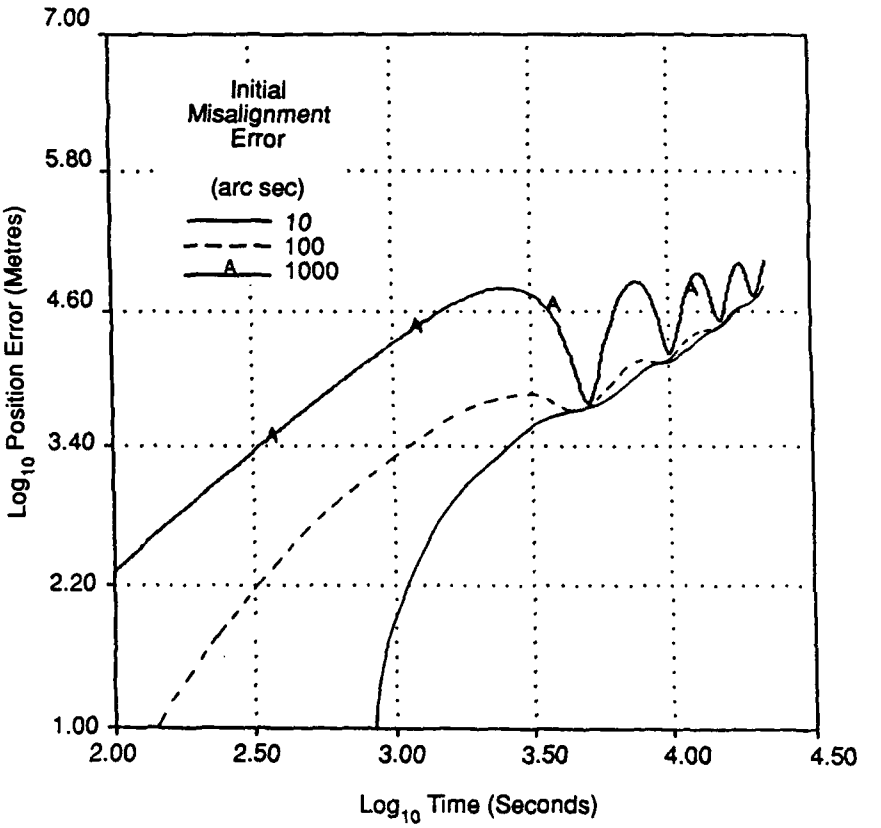

Figure 5. Initial misalignment error

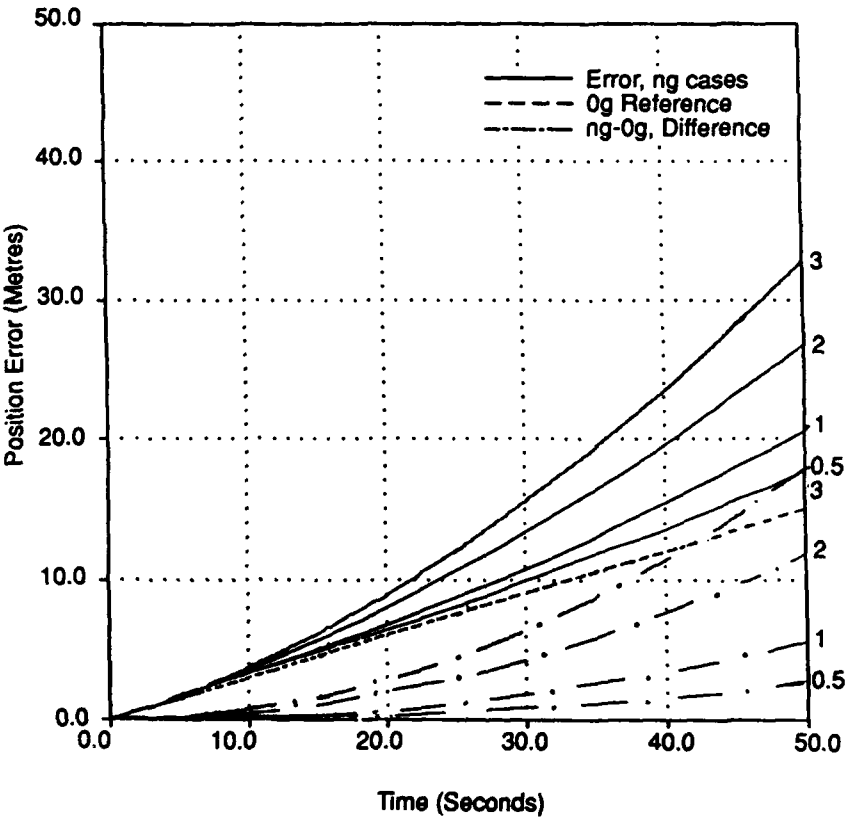

Figure 6. The effect of linear acceleration on position error

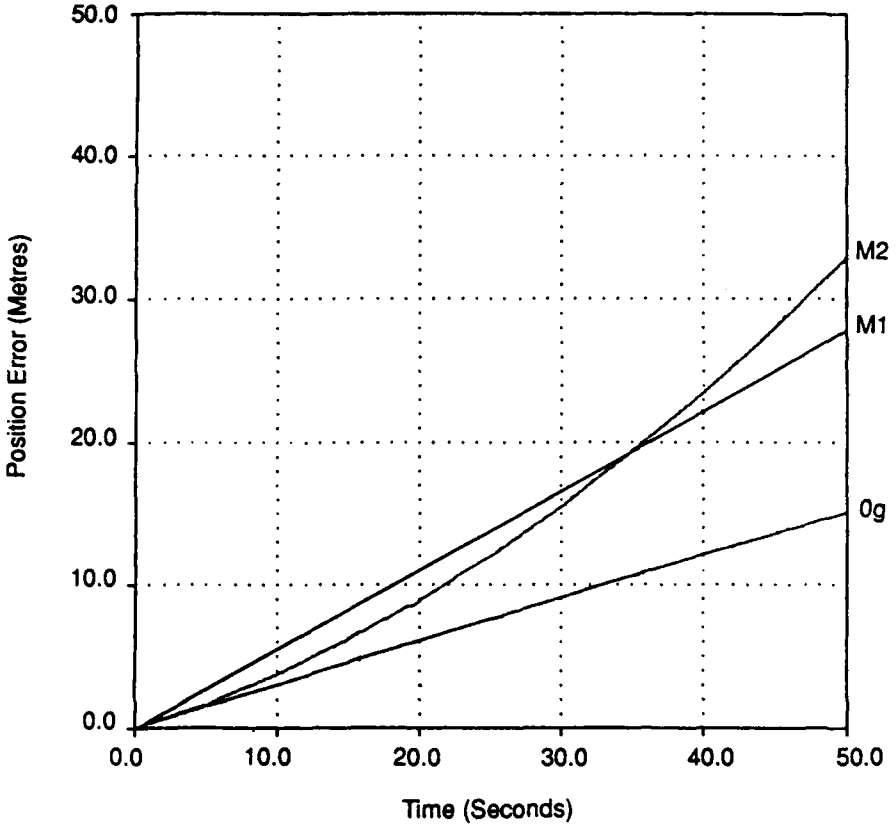

Figure 7. Comparison of M1-M2, radial position errors, under constant linear acceleration

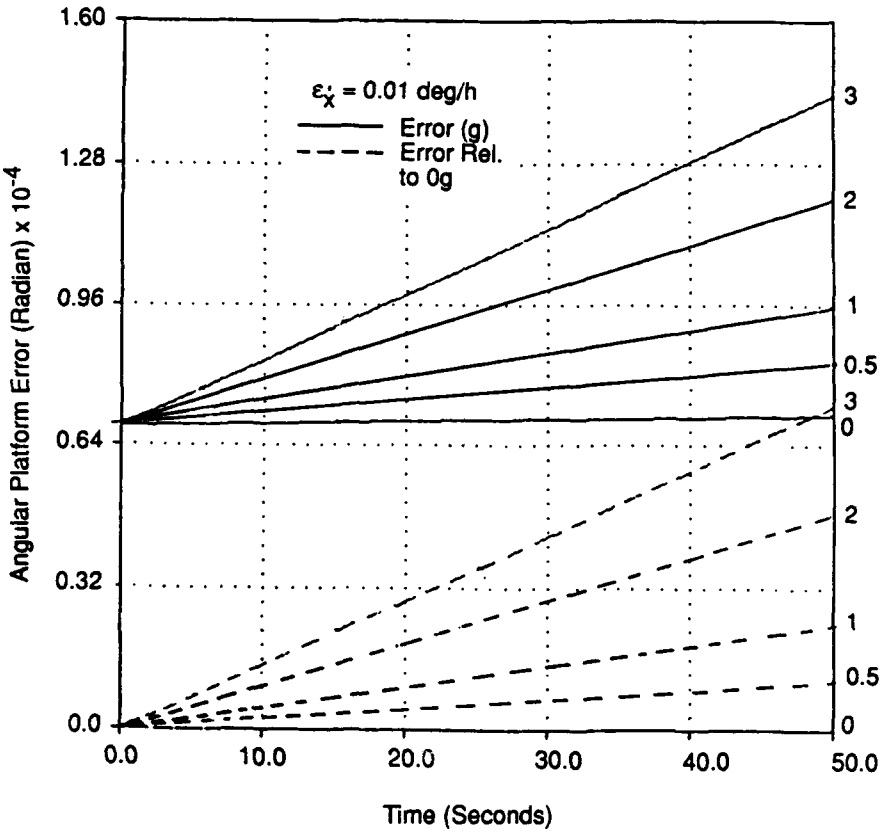

Figure 8. The effect of linear acceleration on platform errors

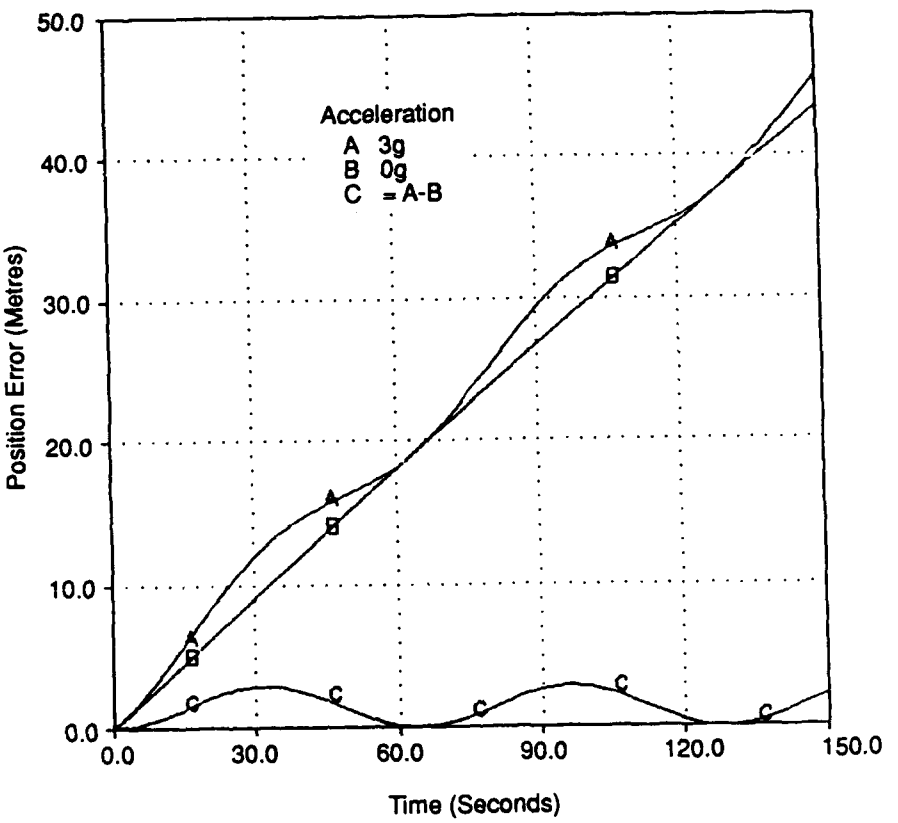

Figure 9. The effect of centripetal acceleration on position error

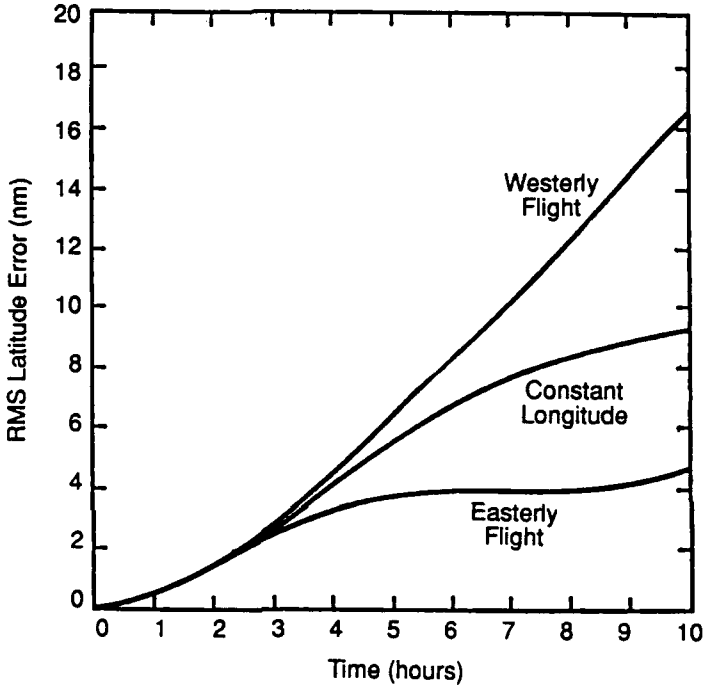

Figure 10. A comparison of RMS latitude error for various flight directions

DISTRIBUTION

	No. of copies
Defence Science and Technology Organisation	
Chief Defence Scientist First Assistant Secretary Science Policy Director General Science Resources Planning and Commercialisation Director General Science and Technology Programs Director General Space and Scientific Assessements Assistant Secretary Science Corporate Management Assistant Secretary Development Projects	1
Counsellor, Defence Science, London	Cnt Sht Only
Counsellor, Defence Science, Washington	Cnt Sht Only
Defence Science Representative, Bangkok	Cnt Sht Only
Scientific Adviser, Defence Research Centre, Kuala Lumpur	Cnt Sht Only
Scientific Advisor to Defence Central	1
Weapons Systems Research Laboratory	
Director, Weapons Systems Research Laboratory	1
Chief, Combat Systems Division	1
Chief, Maritime Systems Division	1
Chief, Ordnance Systems Division	1
Chief, Guided Weapons Division	1
Research Leader, Combat Systems	1
Head, Combat Systems Effectiveness	1
Head, Combat Systems Integration	1
Head, Combat Systems Technology	1
Head, Operations Research	1

Head, Range Measurements Branch	1
Authors	2
Aeronautical Research Laboratory	
Director, Aeronautical Research Laboratory	1
Electronics Research Laboratory	
Director, Electronics Research Laboratory	1
Materials Research Laboratory	
Director, Materials Research Laboratory	1
Surveillance Research Laboratory	
Director, Surveillance Research Laboratory	1
Libraries and Information Services	
Librarian, Technical Reports Centre, Defence Central Library, Campbell Park	1
Document Exchange Centre, Defence Information Services for:	
Microfiche copying	1
United Kingdom, Defence Research Information Centre	2
United States, Defense Technical Information Centre	2
Canada, Director, Scientific Information Services	1
New Zealand, Ministry of Defence	1
National Library of Australia	1
Main Library, Defence Science and Technology Organisation Salisbury	2
Library, Defence Science and Technology Organisation Sydney	1
Library, Materials Research Laboratory	1

Library, DSD, Melbourne	1
Australian Defence Force Academy Library	1
British Library, Document Supply Centre	1
Department of Defence	
Director of Departmental Publications	1
Joint Intelligence Organisation (DSTI)	1
Navy Office	
Navy Scientific Adviser	Cnt Sht Only
Army Office	
Scientific Adviser - Army	1
Air Office	
Air Force Scientific Adviser	1
Director of Systems Engineering A - Airforce	1
Director of Systems Engineering B - Airforce	1
Spares	3
Total number of copies	44

DOCUMENT CONTROL DATA SHEET

Security classification of this page : UNCLASSIFIED

1 DOCUMENT NUMBERS	
AR Number :	AR-006-454
Series Number :	WSRL-TM-30/90
Other Numbers :	

2 SECURITY CLASSIFICATION	
a. Complete Document :	Unclassified
b. Title in Isolation :	Unclassified
c. Summary in Isolation :	Unclassified

3 DOWNGRADING / DELIMITING INSTRUCTIONS

4 TITLE

A GENERIC INERTIAL NAVIGATION SYSTEM MODEL FOR COMPUTER SIMULATION STUDIES

5 PERSONAL AUTHOR (S)

D.A.B. Fogg and
R.T. Janus

6 DOCUMENT DATE

September 1990

7	
7. 1 TOTAL NUMBER OF PAGES	31
7. 2 NUMBER OF REFERENCES	16

8 8. 1 CORPORATE AUTHOR (S)

Weapons Systems Research Laboratory

8. 2 DOCUMENT SERIES and NUMBER
Technical Memorandum 30/90

9 REFERENCE NUMBERS	
a. Task :	AIR 86/166
b. Sponsoring Agency :	DSTO

10 COST CODE

11 IMPRINT (Publishing organisation)

Defence Science and Technology Organisation

12 COMPUTER PROGRAM (S) (Title (s) and language (s))

13 RELEASE LIMITATIONS (of the document)

Approved for Public Release.

Security classification of this page : UNCLASSIFIED

Security classification of this page : UNCLASSIFIED

14 ANNOUNCEMENT LIMITATIONS (of the information on these pages)

No limitation

15 DESCRIPTORS

a. EJC Thesaurus Terms: Inertial navigation; F-111C aircraft

b. Non - Thesaurus Terms: Pave Tack system

16 COSATI CODES

170703

17 SUMMARY OR ABSTRACT
(if this is security classified, the announcement of this report will be similarly classified)

(U) A number of Inertial Navigation System (INS) models ranging from simple forced harmonic oscillator models to three-gyro, three-accelerometer systems were studied to ascertain a compromise between accuracy and computation time on the one hand and model complexity suitable for use in avionics system models for effectiveness studies on the other. INS position and orientation errors for various cruise and acceleration conditions were predicted by these models and the results shown graphically. The importance of various INS characteristics has been determined and the effects of the relevant error sources have been isolated and their propagation in time plotted.

Security classification of this page : UNCLASSIFIED